

REGULAR PAPER

Measurement of mechanical properties of liquid by observing droplet oscillation on substrates

To cite this article: Satoshi Ishida *et al* 2022 *Jpn. J. Appl. Phys.* **61** SG1064

View the [article online](#) for updates and enhancements.

You may also like

- [Erratum: "The Influence of Surface Binding Energy on Sputtering in Models of the Sodium Exosphere of Mercury" \(2022, PSJ, 3, 139\)](#)
Rosemary M. Killen, Liam S. Morrissey, Matthew H. Burger et al.
- [Editorial: Focus issue on machine learning for neuromorphic engineering](#)
Melika Payvand, Emre Neftci and Friedemann Zenke
- [Radiation tolerance of the MUX64 for the High Granularity Timing Detector of ATLAS](#)
C. Wang, Z. Xu, X. Huang et al.



Measurement of mechanical properties of liquid by observing droplet oscillation on substrates

Satoshi Ishida^{1*}, Mika Iga¹, Shujiro Mitani², and Keiji Sakai^{2,3}

¹Research & Development, Nippon Paint Holdings Co., Ltd., Shinagawa, Tokyo 140–8675, Japan

²Institute of Industrial Science, The University of Tokyo, Meguro, Tokyo 153–8505, Japan

³Graduate School of Engineering, The University of Tokyo, Bunkyo, Tokyo 113–8656, Japan

*E-mail: satoshi.ishida@nipponpaint.jp

Received October 29, 2021; revised January 13, 2022; accepted January 17, 2022; published online May 31, 2022

In this paper, we introduce a method to measure the surface tension of a droplet on a solid substrate by observing the resonance oscillation excited by applying Maxwell stress using electric field tweezers in a noncontact manner. Additionally, we measured the frequency spectrum of the oscillation amplitude using a stroboscopic imaging technique. The resonance frequency of the droplet was inversely proportional to the 3/2th power of the droplet radius, with a contact angle of approximately $\pi/2$ rad. The acquired result is in good agreement with the theory derived by extending the established formula for a free-sphere droplet. Furthermore, the contact angle dependence of the resonance frequency can be qualitatively explained based on the behavior of waves on a confined liquid surface. © 2022 The Japan Society of Applied Physics

1. Introduction

Surface tension is one of the most important liquid properties in microscopic and high-speed industrial applications, including spray paint coatings and inkjets. For example, in spray paint coating processes, the wetting is dominated by the surface tension and viscosity of the paint immediately after a droplet impacts the substrate. Various studies have been carried out on the viscosities of paints,^{1–4)} while only a few have been carried out on the surface tension, considering that solvent-borne paints are designed to possess sufficiently low surface tensions to form an excellent film appearance. Therefore, measurements were carried out to determine whether the surface tension was sufficiently small. In recent years, the surface tension of paints has attracted considerable attention owing to water-borne paints, which exhibit higher surface tensions⁵⁾ and have become the mainstream for eco-friendly applications^{6,7)} compared to solvent-borne paints. Although several studies have been carried out on measurement methods for the surface tensions of paints,^{8,9)} sufficiently accurate values have not been obtained.

Usually, the Wilhelmy^{10–12)} and du Noüy methods are employed to determine the static surface tension by the drawing force applied to the plate or ring by the surface tension. However, the measured value was affected by the viscosity. As a result, a period over 1 h is required for the paint viscosity ($>10^4$ mPa s) to reach the equilibrium meniscus form of surface tension. Therefore, these methods are not feasible in ordinal industrial processes.

The maximum bubble pressure method^{13–15)} is employed to obtain the dynamic surface tension, which is determined by the pressure of a gas bubble emitted into the liquid from the capillary nozzle. However, the viscosity of the surrounding liquid contributes to the pressure, which increases the measured value.

A method for measurement of the dynamic surface tension by analyzing the oscillation of a flying droplet was also proposed.^{16,17)} In this method, droplets are emitted into the air from a nozzle, which then travel with oscillation after the initial deformation of the droplet from the equilibrium shape of a sphere. The density of air is sufficiently low, which does not disturb the eigen-oscillation of the droplet. The surface

tension was determined by observing the resonance frequency of the droplet oscillation with a high time resolution using the stroboscopic method. The emission time of the strobe light with a duration shorter than 100 ns gradually shifted from the origin of the droplet injection. However, this method requires a stable reproducibility for every droplet emission, which is difficult to achieve for paints owing to their high spinnability. Furthermore, airborne droplets are difficult to generate in paints.

In this study, we attempted to observe the oscillation phenomenon of a liquid droplet on a solid substrate. Although the resonant oscillation frequency of the partial sphere droplet on the substrate should be a function of the surface tension, it is challenging to excite the oscillation of a small droplet, considering that the mechanical contact of a transducer with a droplet can result in severe deformations from the partial sphere. Experiments have been carried out to excite droplet oscillation on solid substrates using surface acoustic waves.^{18,19)} In these experiments, we used the electric field tweezers technique to extend the types of solid materials. As described below, this method can selectively excite the symmetric mode with respect to the azimuth angle.

There is no formula to relate the oscillation frequency of the droplet on a flat substrate to the surface tension for an arbitrary contact angle. Strani et al. analyzed the oscillation of a liquid droplet in partial contact with a solid substrate with a partial spherical concave.²⁰⁾ The calculation showed a good agreement with the experimental results obtained by Bisch by observation of a liquid droplet placed on a spherical support. However, the preparation of a spherical concave for droplets smaller than millimeter is difficult for practical industrial measurements.

In this study, we analyze the relationship between the surface tension and resonance frequency of a liquid droplet on a flat solid substrate, which is important for application in actual spray coating processes. First, we observed the behavior of a droplet on a substrate with a contact angle of approximately $\pi/2$ rad, while assuming that it is a hemisphere, considering that the resonance frequency of free oscillation is almost equal to the higher mode of a sphere.²¹⁾ Moreover, we analyzed droplets with a wide range of contact angles. We provide a quantitative discussion on the dependence of the resonance frequency on the contact angle.

2. Experimental methods

We summarize the theory of free oscillation of a spherical droplet in air. The frequency of oscillation is determined by the surface tension of the liquid, which functions as a restoring force, and density as a mass. Further, we discuss the droplet oscillation, which has cylindrical symmetry with respect to the latitude direction.

The oscillation can be regarded as a surface wave traveling to the sphere surface. The resonance frequency is determined by the resonance condition, where the phase of the wave changes by $2l\pi$ for a round trip along the meridian, where l is an integer. The resonance angular frequency of the droplet oscillation is

$$\omega_l = \sqrt{\frac{l(l-1)(l+2)\sigma}{\rho R^3}}, \quad (l \geq 2) \quad (1)$$

where σ is the surface tension, ρ is the density, and R is the droplet radius.²²⁾ The oscillation between the prolate and oblate spheroids is represented by $l=2$. The fundamental mode indicating the oscillation between the prolate and oblate spheres is expressed by $l=2$, which indicates that the length of the great circle of the spherical droplet is twice the wavelength. For a hemisphere on a solid substrate, the boundary condition represents that the amplitude at the droplet contact line and substrate is fixed; i.e. half of the length of the great circle is $3/2$ of the wavelength, denoted as $l=3$. This assumption does not provide a strict solution for the oscillation of a hemisphere, in which the boundary condition should be that the flow velocity is zero in all regions of the contact plane between the droplet and substrate.

We introduce an experimental system. We used the electric field tweezer system^{23–26)} to remotely apply stress to excite the harmonic oscillation of the droplet on a substrate. When an electric field is applied to the interface between two substances with different dielectric constants, the Maxwell stress acts in the direction normal to the interface into the medium with a lower dielectric constant.

Furthermore, we used a stroboscopic technique^{17,27,28)} to observe the high-speed motion of the droplet. The typical droplet size used in this experiment was approximately 1 mm. The expected oscillation frequency was in the range of 10^2 Hz, whereas a time resolution better than $100 \mu\text{s}$ was used. We employed a stroboscopic observation, with a strobe light synchronized to the signal of the harmonic electric field, instead of a high-speed camera. The duration of the light was smaller than $1 \mu\text{s}$, which provided a satisfactory time resolution for the observation. Experimentally, the stroboscope is illuminated from the phase origin of the harmonic excitation signal of the electric field with a certain delay. We acquired a slow-motion video of the droplet behavior by gradually sweeping the delay.

Figure 1 shows a schematic of the experimental setup. Using a metal needle, an electric field was generated at a high voltage and set just above the center of the droplet plate, which excited the deformation of the droplet with Maxwell stress. The solid substrate was set on a plane metal electrode conducted at the ground level.

The electric field of this experiment had rotational symmetry, whose axis coincided with that of the droplet.

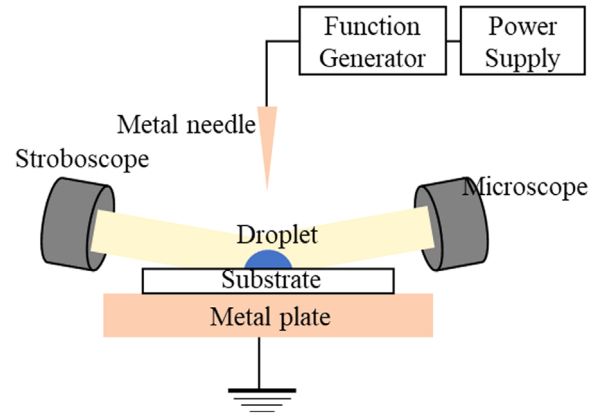


Fig. 1. (Color online) Schematic of the experimental setup. For strong lighting, the stroboscope light is focused and irradiated to the droplet.²¹⁾

Hereafter, we use the cylindrical coordinates, where r denotes the distance from the center axis. The surface displacement $\xi(r)$ owing to the Maxwell stress is expressed by²³⁾

$$\sigma \Delta_S \xi(r) - \rho g \xi(r) + f(r) = 0, \quad (2)$$

where $f(r)$ is the distribution of the Maxwell stress, g is the gravitational acceleration, and Δ_S is the two-dimensional Laplacian operator along the surface. The effect of the Maxwell stress appeared as a summation of the amplitude of the surface displacement and additional surface curvature.

For the excitation of the droplet oscillation, the boundary condition was modified by considering the initial curvature of the surface. However, this does not influence the excitation of the resonance oscillation. The deformation mode was selected based on the symmetry and boundary condition of the droplet.

The needle tip must be sufficiently close to the surface to induce an adequate displacement for an image analysis. Practically, the distance should be smaller than 1 mm. It is also necessary to maintain a distance to ensure that the droplet and needle do not contact during vibration. Therefore, the needle was set at an appropriate distance from the top of the droplet for each experiment. The frequency $f (= \omega/2\pi)$ range of the measurement was 10–400 Hz.

3. Results and discussion

First, we demonstrate the dynamic behavior of a droplet on a water-repelling glass plate, assuming that it is a hemisphere. Ethylene glycol and distilled water were used as samples with contact angles of 95° on the plate. We assumed a value of approximately $\pi/2$ rad. Table I summarizes the density, surface tension, and viscosity of each liquid. The droplet volume was set in the range of 0.5 – $12 \mu\text{l}$ by changing the sampling amount using a microsyringe.

Figure 2 shows photographs of the oscillation of the ethylene glycol droplet during a quarter cycle of the sinusoidal application of Maxwell stress. The contact line

Table I. Fluid properties at laboratory conditions.

Property	Unit	Ethylene glycol	Distilled water
Density ^{34,35)}	kg m^{-3}	1.1×10^3	1.0×10^3
Surface tension ^{36,37)}	N m^{-1}	4.8×10^{-2}	7.3×10^{-2}
Viscosity ³⁸⁾	Pa s	2.0×10^{-2}	1.0×10^{-3}

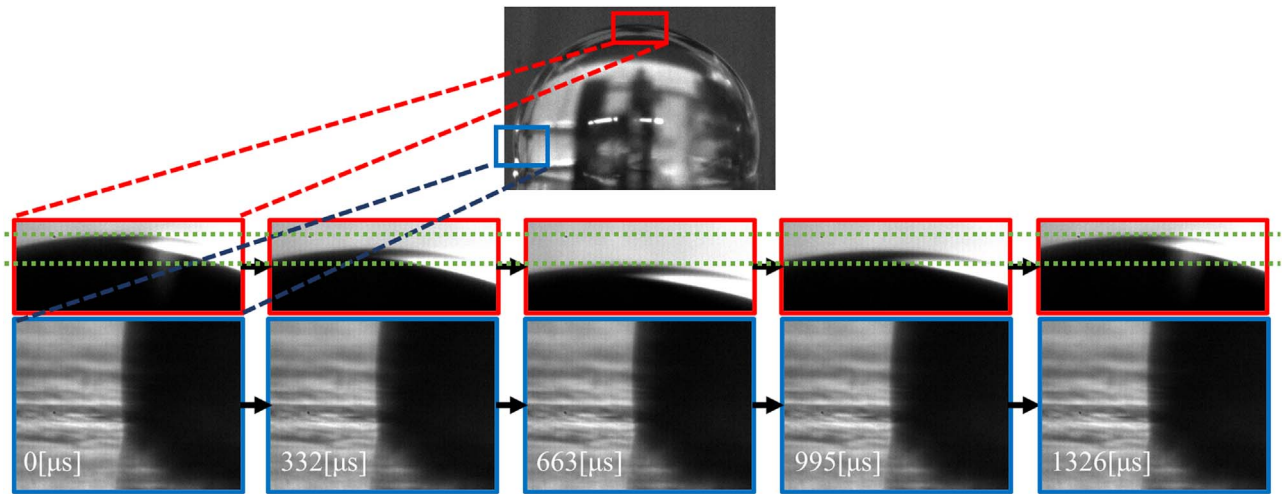


Fig. 2. (Color online) Photograph of the ethylene glycol droplet per quarter cycle in the sinusoidal electric field.²¹⁾ (Voltage angular frequency = 754 s^{-1} , Droplet height = 1.2 mm).

with the substrate is fixed while the top of the droplet oscillates. Furthermore, there are two nodes on the meridian crossing the top of the droplet according to the photographs of the entire oscillating droplet. These results indicate that the droplet oscillation at a contact angle of $\pi/2$ rad on the substrate can be considered as the mode denoted by the index $l = 3$ in Eq. (1). The image analysis of droplet oscillation was effective in assigning the oscillation mode.

The time dependence of the height of the droplet top was obtained through the image analysis. The oscillation amplitude $A(\omega)$ was determined to be half of the change in height. Figure 3 shows the angular frequency dependence of the normalized amplitude $A(\omega)/A_{\text{max}}$ obtained for the distilled water (a) and ethylene glycol (b) droplets, where A_{max} is the maximum amplitude. The resonance frequency increases as the droplet radius decreases. Additionally, the width of the peak of the distilled water droplet was smaller than that of ethylene glycol, which can be attributed to the decay of oscillation through viscous energy dissipation. The peak width and decay of the surface wave are discussed below.

We consider the effects of gravity and viscosity. The gravity contributes to the resonance frequency if the radius of the droplet is larger than the capillary length, which is expressed by $(\sigma/\rho g)^{1/2}$ and is approximately 3 mm for water. The maximum radius is 2.1 mm in this experiment, and thus we ignore the contribution of gravity. In addition, the viscosity modifies the resonance frequency above the MHz region.²⁹⁾ The frequency range of this experiment is considerably lower, and thus we neglected the contribution of viscosity to the resonance frequency.

As shown in Fig. 4, we determined the resonance frequency of the spectrum peak as a function of the droplet radius. The contact angle was not exactly $\pi/2$. The radius R was determined by the droplet height. The dashed and dotted lines indicate the results of Eq. (1) with a mode index of $l = 3$. The resonance frequency was proportional to $R^{-3/2}$, which is in good agreement with the theoretical results. The contact angle was not accurately $\pi/2$; hence, we could only analyze the power law between the droplet size and resonance frequency.

The resonance frequency of distilled water was higher than that of ethylene glycol, which can be attributed to the

differences in surface tension and density. Moreover, the ratio between them of 0.71 is in good agreement with the theoretical prediction of 0.77 obtained by Eq. (1), together with the values of the surface tensions and densities.

Notably, these theoretical values were calculated assuming that the droplet on the substrate was a hemisphere, although the actual contact angles were not $\pi/2$ rad. Further, we investigated the contribution of the contact angle to the resonance frequency. To measure the resonance frequency of the droplet by changing the contact angle, we prepared flat substrates of different materials in addition to a water-repelling glass plate, as shown in Table II. We measured the frequency spectrum of the oscillation and determined the resonance frequencies of the ethylene glycol droplets with a constant volume on these substrates. The contact angles obtained by the image analysis were in the range of 0.72–1.7 rad.

Figure 5 shows the experimentally obtained resonance frequencies as a function of the contact angle. The droplet volumes were identical. The resonance frequency exhibited a maximum at approximately $\pi/2$.

Below, we explain the contact angle dependence of the resonance frequency in terms of the resonance of the surface tension waves in a confined surface area.

As mentioned above, the boundary condition of the surface waves confined in a droplet on the substrate indicates that the displacement is fixed at the circular contact line. In addition, the surface displacement exhibited cylindrical symmetry. Hereafter, we discuss the condition under which the droplet volume is kept constant and the contact angle is variable. The resonance condition can be determined such that the length of the meridian crossing the top of the droplet is the same as the length of $3/2$ of the wavelength.

Considering that the droplet volume is maintained as V_0 , the radius of curvature of the droplet $R(\theta_c)$ is a function of the contact angle θ_c , expressed by

$$V_0 = \pi R^3 \left(\frac{1}{3} \cos^3 \theta_c - \cos \theta_c + \frac{2}{3} \right). \quad (3)$$

The meridian length L is expressed as $L = 2 \theta_c R(\theta_c)$, while the resonance frequency varies according to $\omega_l \sim \alpha (\sigma/\rho)^{1/2} L^{-3/2}$, where α is a constant, as the length L is an integer multiple of

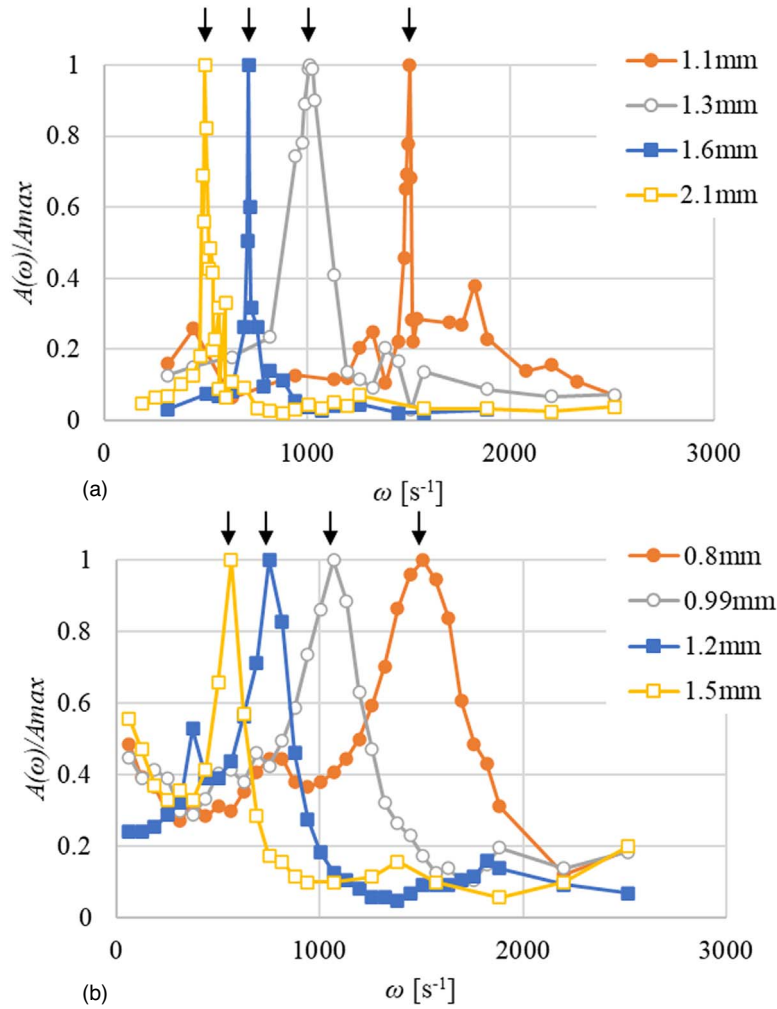


Fig. 3. (Color online) Dependence of angular frequency on the normalized amplitude of distilled water (a) and ethylene glycol (b). The arrows indicate the resonance frequency at each condition. Each explanatory note indicates the height of each droplet measured through image analysis.²¹⁾

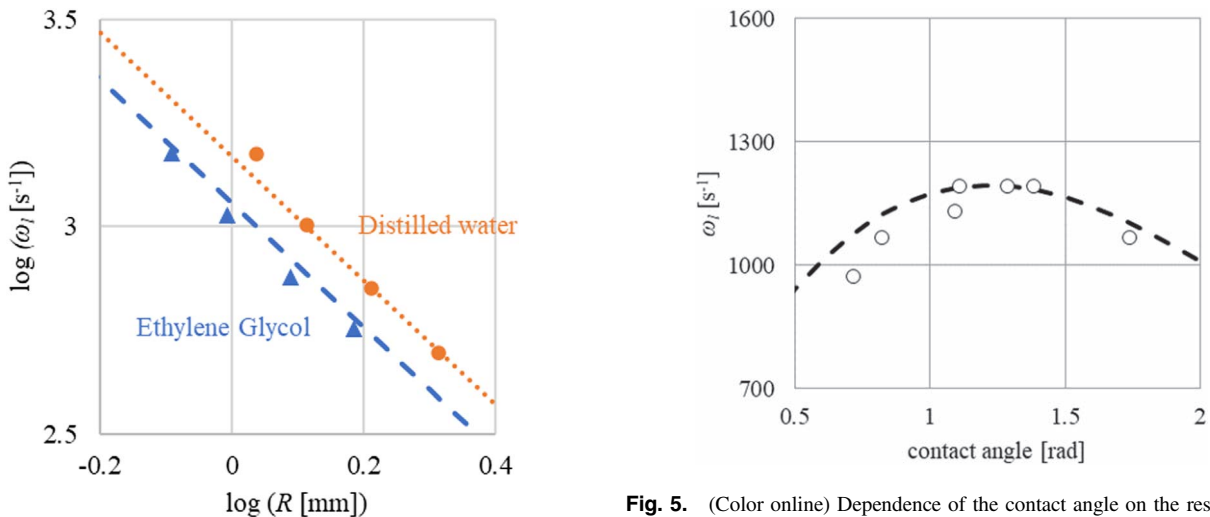


Fig. 4. (Color online) Dependence of R on the resonance frequency. The circles and triangles indicate the measured values for distilled water and ethylene glycol, respectively. The dashed line and dotted line indicate the theoretical values for distilled water and ethylene glycol, respectively.²¹⁾

Fig. 5. (Color online) Dependence of the contact angle on the resonance frequency of the ethylene glycol droplet. The circles and dashed line indicate the measured and theoretical values, respectively.

the half-wavelength of the standing wave. The frequency of the surface wave with a wavelength of λ is $(8\pi^3 \sigma \rho)^{1/2} \lambda^{-3/2}$.²²⁾ The qualitative dependence of ω_l on the contact angle can be determined using the above equations, indicated by the dashed

line in Fig. 5, which is drawn by adjusting the value of α to reproduce the experimental result. The above rough theory of wave propagation predicts that the wavelength exhibited a minimum and that the resonance frequency exhibited a maximum at approximately $\pi/2$, which is in good agreement. This behavior is derived from the simple fact that the length of the arc

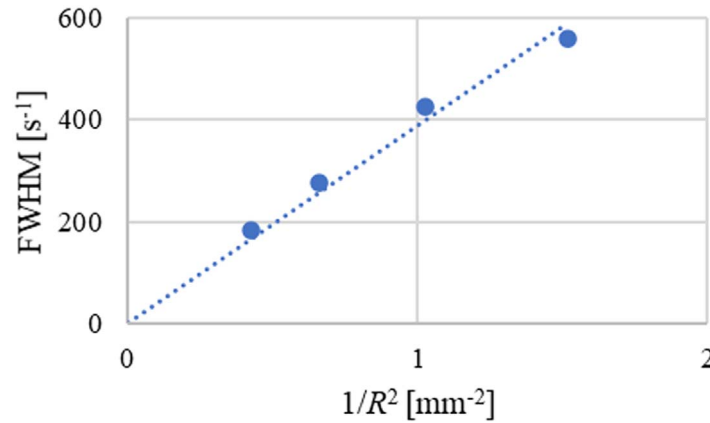


Fig. 6. (Color online) FWHM plotted against $1/R^2$ for ethylene glycol.²¹⁾

Table II. Substrate and contact angle of ethylene glycol.

Substrate	Glass	Steel painted undercoat	Steel painted basecoat
Contact angle [rad]	0.72	0.82	1.1
Substrate	Polystyrene	Polymethylmethacrylate	Polypropylene
Contact angle [rad]	1.1	1.3	1.4

determining the wavelength of the resonance wave has a minimum at approximately $\theta_c = 1.22$ rad.

Although a detailed discussion is required to accurately understand the oscillation of droplets on substrates, the present results provide a useful knowledge about the oscillation. First, Fig. 5 shows that the resonance frequency is not very sensitive to the contact angle around the right angle; i.e. the surface tension can be determined accurately even though the contact angle of actual industrial systems is scattered around the right angle. Second, the validity of our rough analysis shows that the phenomenon of droplet oscillation can be treated as the resonance of the surface tension waves.

Finally, we briefly discuss the peak width of the resonance curves based on the decay of surface waves owing to viscosity. Viscosity is an essential liquid property in microscopic and high-speed industrial applications. The oscillation of a free droplet after being emitted from the nozzle is damped by the liquid viscosity,^{30,31)} where the damping constant Γ is proportional to $\eta/\rho R^2$, where η is the viscosity of the liquid. The oscillation decay appeared as the peak width in the frequency spectrum.^{32,33)} The energy dissipation by the substrate is negligible because of the sufficiently high modulus (Young modulus $> 10^3$ MPa). Figure 6 shows the full width at half maximum of the resonance peak plotted against $1/R^2$ for the ethylene glycol droplet. The experimental results are in good agreement with the expected power law. An absolute calculation of the energy dissipation is required to determine the viscosity while changing the contact angle.

4. Conclusions

In this study, we successfully developed a method to remotely excite the resonance oscillation of liquid droplets on a solid substrate using an electric tweezer system. Furthermore, we employed stroboscopic image observation to detect oscillations, which enabled us to confirm the resonance mode.

The resonance frequency was dependent on the droplet radius for distilled water and ethylene glycol. The oscillation of the droplet, with a contact angle of approximately $\pi/2$ rad, behaved similarly to the oscillation of a free spherical airborne droplet at the higher mode of $l = 3$. The resonance frequency was qualitatively consistent with the theory under the assumption that the droplet was a hemisphere.

Additionally, the dependence of the resonance frequency of droplets placed on various substrates on the contact angle was explained by the theory of surface waves in a confined liquid area. The peak width of the resonance frequency provided information on the energy dissipation owing to viscosity.

We believe that these results provide a novel viewpoint for a new method for measurement of the mechanical properties of liquids by observing the droplet oscillation on a flat substrate. However, this experimental data is in agreement with the theoretical results, not quantitatively but qualitatively. Therefore, we will aim to provide a more accurate calculation method for droplet oscillation using hydrodynamic simulations in future studies. In addition, we will soon report a simpler method for the detection of droplet oscillation in industrial processes.

The final aim of this study is to extend the size to the order of micrometers, which is employed in actual industrial processes including spray coating and inkjet printing. A novel method for the emission of microscale droplets of highly viscous liquids has been reported.

- 1) R. R. Myers, *J. Coat. Technol.* **52**, 65 (1980).
- 2) R. Keunings and D. W. Bousfield, *J. Non-Newton. Fluid* **22**, 219 (1987).
- 3) O. Cohu and A. Magnin, *Prog. Org. Coat.* **28**, 89 (1996).
- 4) F. Seeler, C. Hanger, O. Tiedje, and M. Schneider, *J. Coat. Technol. Res.* **14**, 767 (2017).
- 5) M. J. Schnell, *Polym. Mater. Sci. Eng.* **66**, 79 (1992).
- 6) R. R. Harris, *Trans. IMF* **67**, 35 (1989).
- 7) J. Bourne, *Surf. Coat. Int.* **92**, 244 (2009).

- 8) V. P. Janule, *Mod. Paint. Coat.* **89**, 32 (1999).
- 9) A. Bochkarev, M. Hartman, K. Olson, and V. Polyakova, *J. Coat. Technol. Res.* **7**, 347 (2010).
- 10) R. E. Johnson Jr., R. H. Dettre, and D. A. Brandreth, *J. Colloid. Interface Sci.* **62**, 205 (1977).
- 11) R. E. Smith, *Ind. Eng. Chem. Prod. Res. Dev.* **22**, 67 (1983).
- 12) A. Bak and W. Podgorska, *Colloids Surf. A* **504**, 414 (2016).
- 13) N. C. Christov, K. D. Danov, P. A. Kralchevsky, K. P. Ananthapadmanabhan, and A. Lips, *Langmuir* **22**, 7528 (2006).
- 14) N. A. Mishchuk, V. B. Fainerman, V. I. Kovalchuk, R. Miller, and S. S. Dukhin, *Colloids Surf. A* **175**, 207 (2000).
- 15) J. Adelsky, *Tappi J.* **73**, 109 (1990).
- 16) B. Stückrad, W. J. Hiller, and T. A. Kowalewsk, *Exp. Fluids* **15**, 332 (1993).
- 17) T. Ishiwata and K. Sakai, *Appl. Phys. Express* **7**, 077301 (2014).
- 18) S. Yamakita, Y. Matsui, and S. Shiokawa, *Jpn. J. Appl. Phys.* **38**, 3127 (1999).
- 19) K. Miyamoto, S. Nagatomo, Y. Matsui, and S. Shiokawa, *Jpn. J. Appl. Phys.* **41**, 3465 (2002).
- 20) M. Strani and F. Sabetta, *J. Fluid Mech.* **141**, 233 (1984).
- 21) S. Ishida, M. Iga, S. Mitani, and K. Sakai, *Proc. Symp. on UltraSonic Electronics*, 2021, 3Pa2–8.
- 22) V. G. Levich, *Physicochemical Hydrodynamics* (Prentice-Hall, UpperSaddle River, NJ, 1962), p. 591.
- 23) K. Sakai and Y. Yamamoto, *Appl. Phys. Lett.* **89**, 211911 (2006).
- 24) Y. Shimokawa and K. Sakai, *Phys. Rev. E* **87**, 063009 (2013).
- 25) S. Inaba, S. Fujino, and K. Sakai, *Phys. Chem. Glasses-B* **51**, 304 (2010).
- 26) S. Inaba, S. Fujino, T. Kajiwara, and K. Sakai, *J. Soc. Rheol. Jpn.* **39**, 49 (2011).
- 27) D. Hayakawa, T. Hirano, S. Mitani, and K. Sakai, *Jpn. J. Appl. Phys.* **56**, 07JB02 (2017).
- 28) R. Yokota, T. Hirano, S. Mitani, and K. Sakai, *Appl. Phys. Express* **13**, 017001 (2020).
- 29) K. Sakai, P. L. Choi, H. Tanaka, and K. Takagi, *Rev. Sci. Instrum.* **62**, 1192 (1991).
- 30) H. Kutsuna and K. Sakai, *Appl. Phys. Express* **1**, 027002 (2008).
- 31) T. Yamada and K. Sakai, *Phys. Fluids* **24**, 022103 (2012).
- 32) I. Egry, H. Giffard, and S. Schneider, *Meas. Sci. Technol.* **16**, 426 (2005).
- 33) K. Higuchi, M. Watanabe, R. K. Wunderlich, and H. J. Fecht, *J. Jpn. Soc. Microgravity. Appl.* **24**, 169 (2007).
- 34) Fujifilm: Safety data sheet. W01W0105-0098 JGHEEN, <https://labchem-wako.fujifilm.com/sds/W01W0105-0098JGHEEN.pdf>.
- 35) Fujifilm: Safety data sheet. W01W0116-0824 JGHEEN, <https://labchem-wako.fujifilm.com/sds/W01W0116-0824JGHEEN.pdf>.
- 36) J. J. Jasper, *J. Phys. Chem. Ref. Data* **1**, 842 (1972).
- 37) N. B. Vargaftik, B. N. Volkov, and L. D. Voljak, *J. Phys. Chem. Ref. Data* **12**, 817 (1983).
- 38) G. J. Janz, *J. Phys. Chem. Ref. Data* **4**, 877 (1975).